A STUDY ON THE VALIDITY OF A SEISMIC ANALYSIS METHOD IN CONSIDERATION OF ENTIRE BRIDGE SYSTEMS

Shin-ya Okada[1] and Hiroshi Mitamura[2]

Introduction

Currently, seismic response analysis is often used for the seismic design of bridges in Japan. Simple analysis methods using frames are mainly adopted because of the low analysis costs involved, but the accuracy of these techniques has not been verified, and their uncertainty is eliminated by incorporating a high margin of safety into the results. If the accuracy of these simple analysis methods can be improved, the margin of safety can be reduced to allow downsizing of the entire structure. This is expected to lead to cost savings in the construction of new bridges and in the reduction of repair work for existing bridges.

In cold, snowy areas like Hokkaido, ground constants vary due to ground freezing. However, since current seismic design methods in Japan only model the effects of foundation ground as a simple spring, it is difficult to take the effects of frozen ground into account.

The purpose of this study is to improve current analysis methods to enhance the accuracy of seismic design through dynamic verification, and to present a method for foundation modeling in which the response of foundation ground can be taken into account. The accuracy of modeling methods for seismic response analysis was examined by comparing analysis results and actual records for the Onneto Ohashi Bridge, for which valuable strong-motion seismograph data were obtained during the Hokkaido Toho-Oki Earthquake of 1994.

Overview of the On-neto Ohashi Bridge

The On-neto Ohashi Bridge analyzed in this study is 456.0 m in length, and consists of a main span (a Nielsen-Lohse girder structure with a length of 140.0 m) and a side span (a continuous-steel-girder structure with a length of 4 @ 25.0 m) (Fig. 1).

For the side span of this bridge, seismic-isolation-type rubber bearings with lead plugs were used for the first time in Hokkaido. Table 1 presents the dimensions and materials of these rubber bearings. The effects of seismic isolation act only in the axis direction of bridges, as these rubber bearings are designed to move only in the bridge axis direction, and movement at right angles to this direction is restrained by side blocks. When the bridge was designed, the application of seismic isolation bearings was still rare in Japan, and no design method to consider the energy absorption of bearings had been established. For this reason, it was designed to satisfy design calculation by the seismic coefficient method

[1]Researcher of CERI for cold region, PWRI

[2]Doctor of Engineering, Chief researcher of CERI for cold region, PWRI

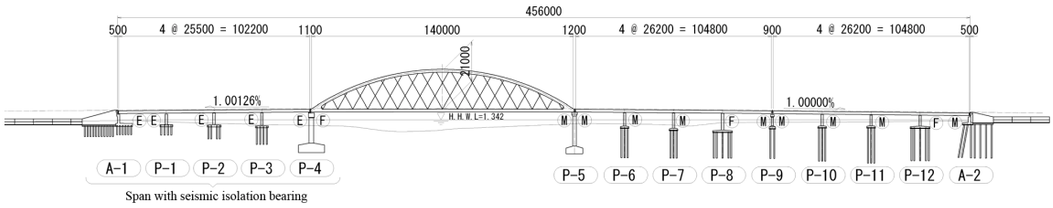

(a) Side view

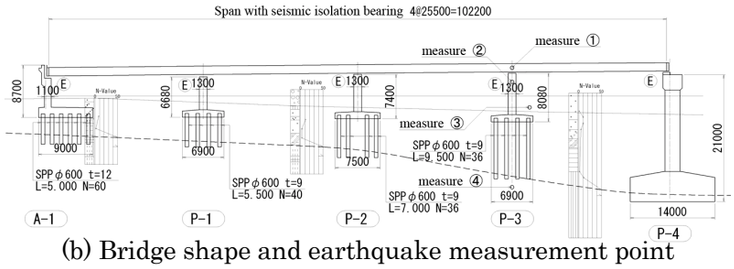

(b) Bridge shape and earthquake measurement point

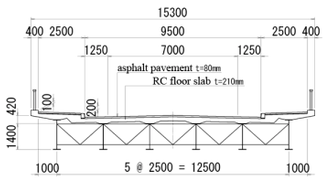

(c) Girder sectional view

Fig.1 On-neto Ohashi Bridge

Table-1 Rubber Bearing Spec

Abutment & Pier		A1 & P4	P1 ~ P3
Bearing		Rubber bearing	Rubber bearing with lead prug
Rubber bearing	Elastic shear coefficient	0.8 N/mm^2	0.8 N/mm^2
	Plane dimensions	300 * 300 mm	450 * 450 mm
	Thickness of rubber layer	9 mm	12 mm
	Layer Number	13	18
	Total Thickness of rubber	117 mm	216 mm
Reinforcing plate	Plane dimensions	280 * 280 mm	430 * 430 mm
	Thickness	3.2 mm	3.2 mm
Lead prug	Diameter & Number	---	145 mm * 1

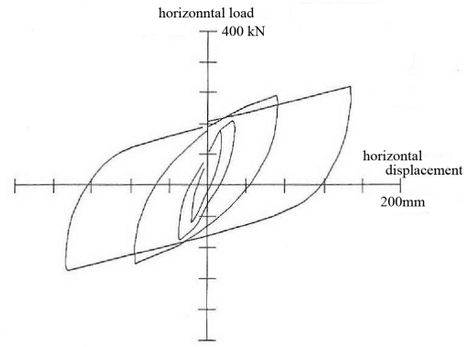

Fig-2 Hysteresis curve of Seismic isolation bearing

and verification by the ultimate earthquake resistance method, even though the seismic isolation effect is not considered in the inertial force value of the substructure. A laboratory test was also conducted to confirm the restoring force characteristics of the seismic isolation bearings. Figure 2 presents an example of a hysteresis curve obtained from a loading test.

The On-neto Ohashi Bridge consists of a main span (a Nielsen-Lohse structure) and a side span (a four-span continuous- steel-girder structure), for which seismic isolation bearings (lead rubber bearings, or *LRB*) are used. These bearings move only in the bridge axis direction, and movement at right angles to the direction is restrained by side blocks with a clearance of 2 mm on each side. Strong-motion seismographs are placed at four points (superstructure, pier top, 1.5 m and 17 m below the ground surface at the P3 pier section). The Hokkaido Toho-Oki Earthquake occurred when only the section with seismic isolation bearings was complete, and seismogram records were obtained.

Strong-motion seismogram records obtained from the Hokkaido Toho-Oki Earthquake of 1994

At the P3 pier section of the side span shown in Fig. 1 (b), acceleration rates in the bridge axis direction, at right angles to the axis direction and in the vertical direction were measured using strong-motion seismographs placed at four measurement points: (1) superstructure, (2) pier top, (3) 1.5 m below the ground surface, and (4) 17 m below the ground surface.

The Hokkaido Toho-Oki Earthquake (M8.1, distance from the epicenter to the bridge: approx. 100 km) occurred on October 4, 1994, when the main span had not been built and only the section with seismic isolation bearings was complete. Strong-motion seismogram records were obtained at different sections of the bridge and in the ground.

Figure 3 illustrates the acceleration time-history waveform in the bridge axis direction obtained during the principal earthquake on October 4. The maximum acceleration of the substructure was smaller than the value at the pier top. This means that, according to past studies in which earthquake behavior was analyzed in detail by spectral analysis of the same waveform, an inertial force reduction effect from the seismic isolation bearings was displayed to a certain degree.

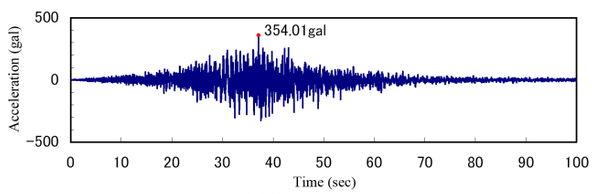

(a) Superstructure

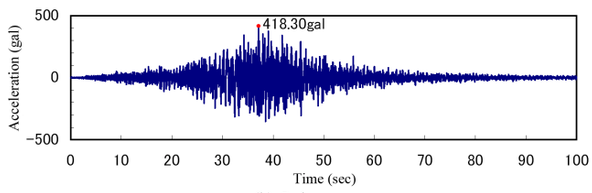

(b) Substructure

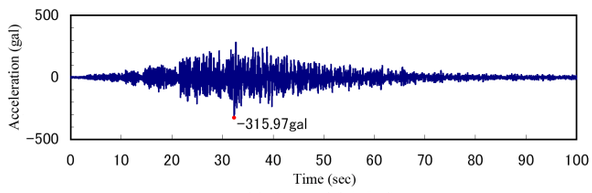

(c) Ground (-1.5m)

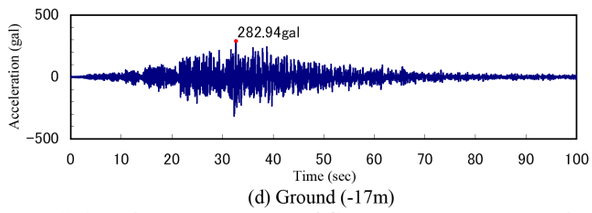

(d) Ground (-17m)

Fig-3 Acceleration Wave of Strong-motion record

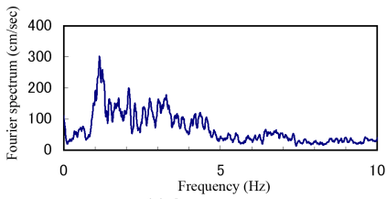

(a) Super structure

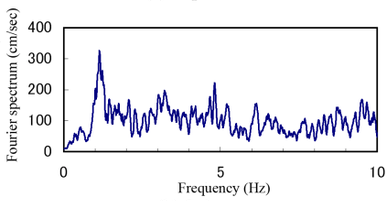

(b) Sub structure

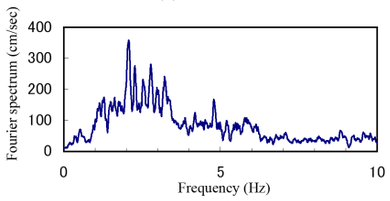

(c) Ground (-1.5m)

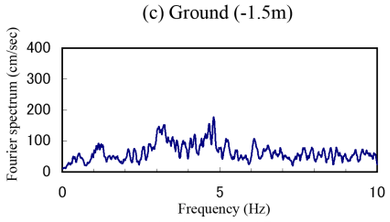

(d) Ground (-17m)

Fig-4 Fourlier spectrum

Figure 4 presents the Fourier spectra of acceleration time-history waveforms obtained at different parts of the bridge and in the ground. The Fourier spectra were smoothed for every 15 plots to clarify the frequency characteristics. Figure 5 shows the rate of transmission found from the ratio of Fourier spectra from 17 m below the ground to the superstructure. The figure indicates the relationship between the degree of amplification and the frequency. The peaks in the figure are thought to be equivalent to the natural frequencies of the superstructure, pier and subsurface ground, which are estimated from the figure to be around 0.99 to 1.19 Hz, 6.56 and 9.08 Hz and 2.04 to 2.44 Hz, respectively.

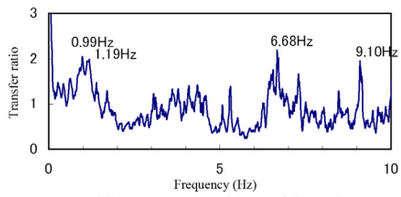

(a) Superstructure / Ground (-1.5m)

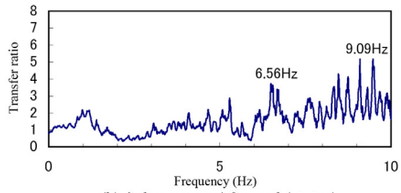

(b) Substructure / Ground (-1.5m)

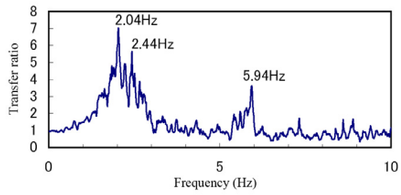

(c) Ground (-1.5m) / Ground (-17m)

Fig-5 Transfer ratio

Analysis model and examination of natural frequencies

(1) Analysis model

The analysis model used for the study was a two-dimensional representation of the bridge's axis direction, since the target bridge was straight and its seismic isolation bearings were designed to move only in the bridge axis direction. The model was a two-dimensional frame rendering of a beam spring-mass system (commonly used in seismic design) without shell, solid or other high-order elements (Fig. 6).

The superstructure was modeled by the elastic beam element at the neutral axis of the composite girder including RC slabs. Each span was divided into six equal parts for the placement of mass points. Horizontal-seismic-force-dispersion-type rubber bearings on

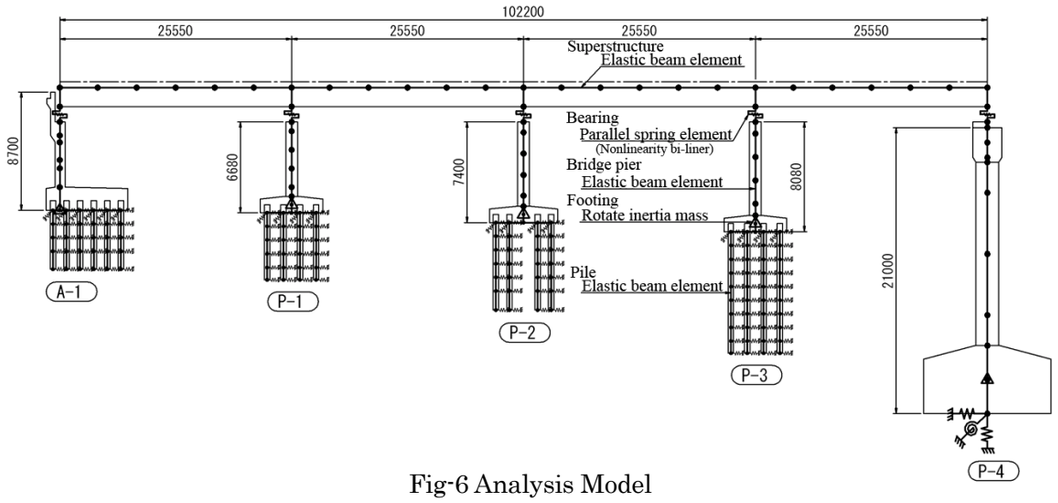

Fig-6 Analysis Model

abutment A1 and pier P4 were modeled as linear spring elements, while seismic isolation bearings on piers P1 – P3 were modeled as nonlinear spring elements with bilinear restoring force characteristics as shown in Fig. 7. The substructure was modeled as an elastic beam element effective for the entire cross section in consideration of the fact that it was not damaged by the Hokkaido Toho-Oki Earthquake, and mass points were positioned by dividing the leg height into five parts. For the foundation structure, dynamic S-R springs (which are expected to improve analysis accuracy according to past study results) were not used. Instead, the piles themselves were modeled as elastic beam elements, and spring values found from the reaction force of the ground in the horizontal and vertical directions were given to the respective nodal points.

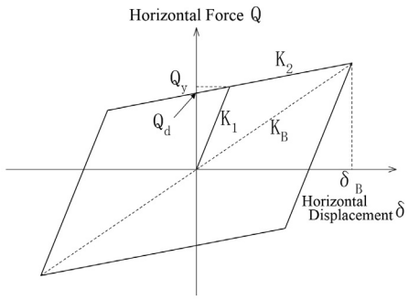

Fig-7 restoring force model of rubber bearing

Table-2 Analysis case

Analysis Case	Difference of the model		Analysis condition
	Impact side block	Ground horizontal spring	Moving axis
Case A	Nothing	Normal	Single axis
Case B	Nothing	1/100	Single axis
Case C	Friction spring	1/100	Double axis

Based on such modeling, the restoring force characteristics of bearings and modeling of the pile foundation ground system were changed to prepare the three types of model used for the study, as presented in Table 2.

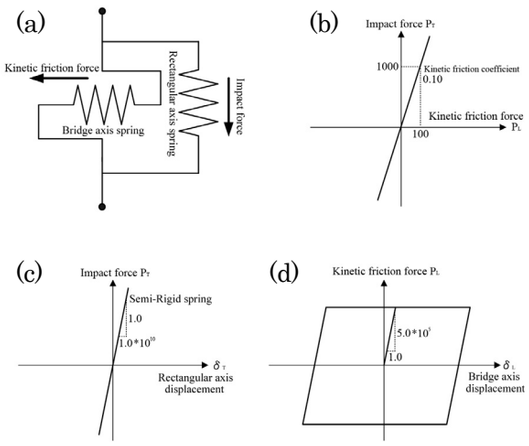

Fig.8 Correlative spring of a collision force and the dynamical friction force

For input earthquake waves, acceleration waveforms in the bridge axis direction recorded at 1.5 m below the ground surface were used. Rayleigh damping, which was used as a viscous damping technique, was set to include the predominant mode during an earthquake based on different orders of mode damping obtained by natural frequency analysis (Fig. 4).

Seismic isolation bearings were modeled as nonlinear spring elements with the bilinear hysteretic characteristics obtained in the laboratory loading test. This is the Case A analysis model studied before, and the two new cases shown in Table 2 were added in this study. In Case B, the piles themselves were modeled as elastic spring elements to give ground spring values to the respective nodal points, and the horizontal spring value was changed to 1/100. This value was adopted on the assumption that the actual ground was softer than the assessment made in a past study, since deformation found in the actual

record of the pier top was considerably greater than the analysis result of Case A. It was therefore attempted to assume softer ground and greater deformation of the foundation in the analysis model. In Case C, freedom at right angles to the bridge axis direction was given to three-dimensionalize Case B. Collision between side blocks and seismic isolation bearings was expressed by bi-directional simultaneous excitation using input earthquake waves, which were acceleration waveforms recorded at 1.5 m below the ground surface in the bridge axis direction and the direction at right angles to the axis. In the bearing section, bi-directional-dependent springs were placed so that the colliding force applied to the side blocks as shown in Fig. 8 and the dynamic-friction force applied in the bridge axis direction would correlate with each other at a dynamic-friction coefficient of 0.10 (assumed value).

Table-3 Comparison of the maximum value (P3)

			Measurement Value	Case A	Case B	Case C
Acceleration	Superstructure	gal (ratio)	354	414 (1.17)	525 (1.48)	374 (1.06)
	Substructure	gal (ratio)	418	494 (1.18)	426 (1.02)	467 (1.12)
Displacement	Superstructure	cm (ratio)	3.3	5.0 (1.52)	8.1 (2.45)	4.9 (1.49)
	Substructure	cm (ratio)	3.6	0.6 (0.17)	5.0 (1.39)	4.8 (1.34)
Bearing	Horizontal Displacement	cm (ratio)	1.5	4.5 (3.00)	5.1 (3.43)	1.5 (1.01)
	Shearing strain	%	7%	21%	24%	7%
	Horizontal force	kN		1563	1750	693

Accuracy verification of dynamic response by seismic response analysis

Table 3 presents a comparison of maximum response values based on the results of seismic response analysis for different cases.

The table shows that the maximum acceleration and maximum displacement of the superstructure in Case A exceeded the measured values, indicating that the superstructure was responding considerably to input seismic waves at the measured level. However, the maximum displacement response at the pier top was less than 20% of the measured value even though the maximum acceleration was greater, indicating less movement of the pier compared with actual measurement. The displacement of the bearing section was also three times as large as the measured value, indicating that the measured value was not reproduced.

Conversely, the maximum displacement of the pier top in Case B, in which the ground was softer, was sufficiently greater than that of Case A and exceeded the measured value. However, both the maximum acceleration and maximum displacement of the superstructure exceeded the measured values considerably, and did not reproduce the superstructure movement. In addition, no improvement was observed in the maximum displacement of the bearing section. This was probably because of the absolute movement of the superstructure due to the greater movement of the entire pier compared with Case A.

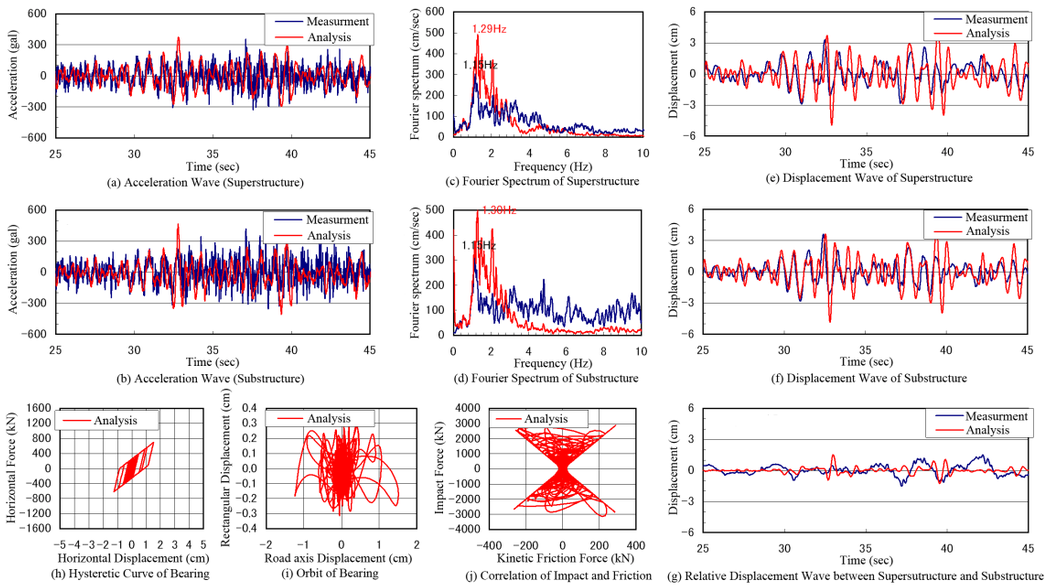

Fig-9 Comparison with an analysis result and the strong-motion record

These results suggest that the stiffness of the bearing section was still underestimated.

Compared with these cases, the maximum response values of almost all items corresponded well with the measured values in Case C, in which the ground was assumed to be soft and the influence of collision with side blocks was taken into account, although the maximum displacement was slightly overestimated.

Figure 9 shows a comparison of dynamic responses by analysis of Case C and strong-motion seismogram records. It can be seen from the figure that the analysis method reproduced the measured waveforms relatively well for both response acceleration and response deformation. It is also clear from the spectra of acceleration that the peak frequencies were almost equal both for the superstructure and the pier top.

A correlation chart of the colliding force and dynamic-friction force also indicates the generation of dynamic friction, which was input in this analysis in consideration of collision with side blocks. It is therefore considered that the main difference between Cases D and E in the analysis results was caused by the friction force generated by the influence of collision with side blocks. This suggests the possible necessity of evaluating the influences of structural details, such as the effects of collision with different sections as discussed in this study, to achieve highly accurate seismic response analysis for seismic isolation bridges.

Conclusion

In this study, the accuracy of seismic response analysis was verified using frame models, and modeling methods for improving accuracy were examined for the Onneto Ohashi Bridge due to the availability of strong-motion seismograph data for different parts of the structure and the ground from the Hokkaido Toho-Oki Earthquake of 1994.

The findings of this study are as follows:

(1) The results of seismic response analysis for the maximum displacement of the pier top were considerably smaller than the results of actual measurement. This was probably because the stiffness of the ground was overestimated in past ground-modeling methods.

(2) The maximum relative displacement of bearings found from seismic response analysis exceeded the measurement results considerably. This was thought to be due to underestimation of the stiffness of bearings in the conventional modeling method for seismic isolation shoes.

(3) To improve the accuracy of the above values, a model in which the foundation was assumed to be softer was used for analysis. While the response of the pier top came closer to the measured values as a result, the response of the superstructure was overestimated.

(4) Examination of the effect of collision between the bearing section and side blocks suggested the possibility of actual collision with side blocks, whose effect was presumed to be relatively strong.

(5) Considering the effect of collision between side blocks and seismic isolation bearings through this analysis method enabled approximate reproduction of the actual behavior of different parts of the bridge.

A possible decrease in the damping effect of seismic isolation bearings under Level 1 earthquake motion was also suggested, although the details could not be clarified in this study. Attention must be paid to this point to enable accurate evaluation of seismic performance. Due to the dynamic interaction between piles and the surrounding ground during an earthquake, the creation of gaps between piles and the ground and a decrease in stiffness were also considered possible under the highly cohesive ground conditions found in this case.